SPACE MOTIONS AND ORBITS OF GLOBULAR CLUSTERS

P. Brosche[1], M. Odenkirchen[1,2], M. Geffert[1], H.-J. Tucholke[1]

[1]Sternwarte Bonn, Auf dem Hügel 71, D-53121 Bonn, Germany
[2]Observatoire de Bordeaux, CNRS/INSU, BP 89, F-33270 Floirac, France

ABSTRACT

Our sample of 15 clusters participates with +40 km s^{-1} in the galactic rotation. A diagram with the two invariants specific axial angular momentum and specific total energy is presented. Eccentricities range from 0.24 to 0.97 with a preference for high values. The observed cluster radii can be regarded as a kind of tidal radii averaged over the orbit.

Key words: globular clusters; orbits; tidal radii.

1. INTRODUCTION

We determined earlier globular cluster proper motions against extragalactic calibrated reference motions (see e.g. Brosche et al. 1991). This paper presents a more comprehensive body of data and its results should be more homogeneous being based on Hipparcos reference motions.

The details of the more observational side of the programme can be found in the contribution of Geffert et al. (1997). Here we want to recall only that precise measurements of good old plates and new plates with epoch differences up to 100 years led to proper motions of 15 globular clusters with typical errors of 0.1 arcsec/cy. In typical distances, this converts into errors of tangential space velocities of ±50 km s^{-1}. Adding radial velocities and photometric distances and taking into account the IAU values of the local standard of rest and of the local galactic rotation (220 km s^{-1}), we arrive at galactocentric space motions at known galactocentric position vectors. This allows to integrate the orbits in a given galactic potential. The resulting orbits and their extremal values permit an individual investigation of the tidal radius problem.

2. THE MOTIONS AND THE INVARIANTS

Again, the individual values can be found in the paper of Geffert et al. (1997). The rotational components range from −127 km s^{-1} to +238 km s^{-1}. The mean is a slight participation in galactic rotation, namely +48 km s^{-1}. Since this can change in time, we anticipate here a result from the orbit integrations below: the mean of the same quantity over 10 Gyr is +41 km s^{-1}. The velocities lead to specific kinetic energies (which are of course *not* invariant) from 0.8×10^4 to 7.1×10^4 (km s^{-1})^2 and to their mean 3.4×10^4 (km s^{-1})^2. All values have been corrected for error dispersions.

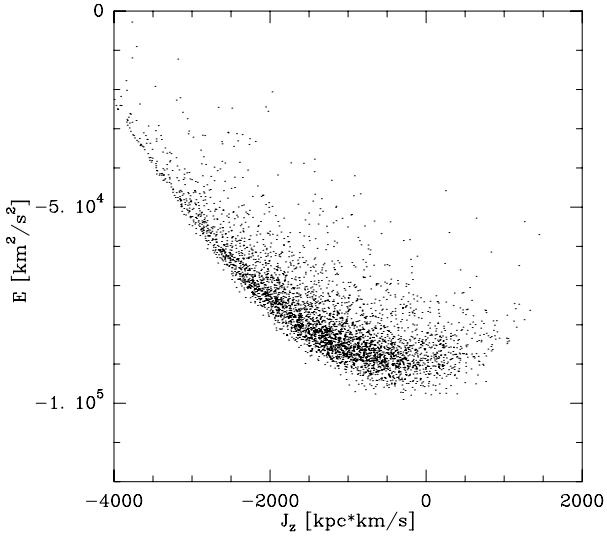

Figure 1. (J_z,E)-distribution of NGC 4147 from the propagation of the observational errors in distance and proper motion.

Under the plausible assumption of an axially symmetric potential, the specific axial angular momentum J_z of the cluster is an invariant. Values range from -1.3×10^3 (km s^{-1}) kpc to $+1.9 \times 10^3$ (km s^{-1}) kpc, with a mean of $+0.25 \times 10^3$ (km s^{-1}) kpc (counted positive in the sense of galactic rotation!).

Any further conclusions have to rest on a model of the galactic potential. We have chosen the one of Allen & Santillan (1991) which seems to be appropriately detailed for the study of halo objects. It is also based on the radial velocities of all globular clusters. By comparing our velocities with the latter one we have

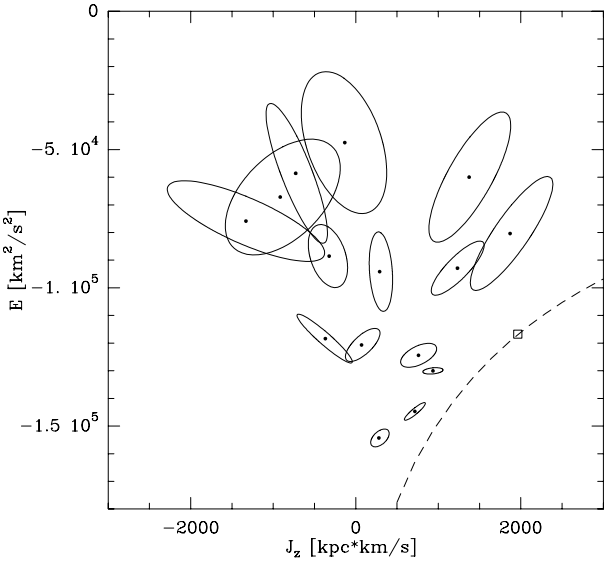

Figure 2. (J_z,E)-distribution of the whole sample.

ensured that they are consistent (any significant difference in the overall size would have produced gross changes in the course of orbital integrations).

We can now compute the specific potential energies as well; combining them with the kinetic energies above leads to specific total energies from -1.5×10^5 (km s^{-1})^2 to -0.5×10^5 (km s^{-1})^2 with a mean of -1.0×10^5 (km s^{-1})^2. The pair (J_z, E) is the most condensed description of our results for a cluster. The propagation of the velocity errors into J_z- and E-errors is not linear and causes strongly non-Gaussian distributions. On the basis of Monte Carlo calculations, an example is given in Figure 1. Keeping this in mind, one can nevertheless determine certain error ellipses; these are provided for the whole sample in Figure 2. For comparison, Figure 2 also shows the location of the Sun (open square) and of circular disk orbits (dashed line).

3. THE ORBITS

Stars moving in the main plane of the Galaxy are subject to relatively large disturbances: there are obviously 'irregular' (i.e. unmodelled) masses there, like e.g. molecular clouds. In contrast, the globular clusters move mainly in the halo where so far we don't have evidence for similar 'irregular' masses. While individual backwards integrations of stellar orbits are made for young stars and times short compared with the age of the Galaxy, it *may be* that our 10 Gyr backwards integrations reveal some characteristics of the real clusters, especially for those with a long period of revolution (defined as time span between consecutive extrema in the galactocentric distance). In general, we want to derive 'recent' individual properties only (for the last few revolutions). Merely for our sample as a whole we believe that a 10 Gyr statistics from our specific start values should be somewhat more realistic than arbitrary start velocities.

Table 1. The orbits.

NGC	R			$\|z\|$		e	top
	max	*min*	$\langle\,\rangle_t$	*max*	$\langle\,\rangle_t$		
	[kpc]			[kpc]			
104	7.9	4.3	6.4	4.3	2.4	0.30	b
362	13.2	0.2	8.8	9.4	2.4	0.97	i
4147	25.8	11.2	19.7	23.4	11.6	0.39	b
5024	40.4	15.8	30.5	38.4	18.5	0.44	b
5272	20.4	6.8	15.1	16.4	8.1	0.55	b
5466	65.3	6.9	46.0	64.8	30.3	0.81	b
5904	22.5	1.3	15.8	19.9	9.4	0.89	b
6205	25.0	4.9	17.8	24.6	11.9	0.67	b
6218	6.5	0.6	4.1	3.4	1.0	0.83	i
6254	5.5	3.4	4.6	2.8	1.6	0.24	b
6341	10.0	3.0	7.3	5.9	3.0	0.54	b
6779	13.5	0.8	9.4	1.4	0.7	0.88	f
6934	39.7	5.9	28.2	36.0	17.2	0.74	b
7078	28.4	7.7	20.6	19.4	9.4	0.57	b
7089	52.7	7.2	36.9	50.9	23.6	0.76	b

Notes: $\langle\,\rangle_t$ = time average; e = orbital eccentricity defined as $(R_{\max} - R_{\min})/(R_{\max} + R_{\min})$; top = topological character classified by b=box-type, f=fish-type, i=irregular.

The paths of the orbits in the comoving meridional sections of the Galaxy are shown in Figure 5 (where they cover a time interval of 3 Gyr). The parameters of the orbits are presented in Table 1. The topological character is clearly tentative. One has to keep in mind that a mathematically 'clean' solution, if possible, would not apply to the real clusters with their finite life time. The physical question is not the orbital character for an infinite time but for 10 to 20 Gyr!

For some of the parameters, rather extreme than average values are important: If the time elapsed since the last transit through the galactic plane is shortest (16 Myrs for NGC 6254), the transit values are most accurate and possible physical consequences should be most distinct. The largest values of the ratio apo- to perigalactic distance will be most informative for the next chapter.

4. TIDAL RADII

From the observed apparent magnitudes and the distances, absolute magnitudes of the clusters are known. Mandushev et al. (1991) have used central velocity dispersions of 32 clusters in order to derive a mass-luminosity-relation with a modest variation of M/L from 2 to 5 along the observed interval. Using this relation, we obtain the masses $M_{\rm cl}$ of column 1 in Table 2 for our clusters. Now it is possible to ask for the influence of the tidal forces on the structure and limitation of the cluster. A limiting boundary can be given in the case of the restricted three-body problem with a circular orbit of the two nonvanishing masses. In the case of a real cluster in a non-circular orbit and with an unknown distribution of the inner motion of its stars, one can at least ask for the distance from cluster center, at which (at any given galactocentric position of the cluster) the combined acceleration from tidal forces $\partial^2\Phi/\partial R^2$ of the

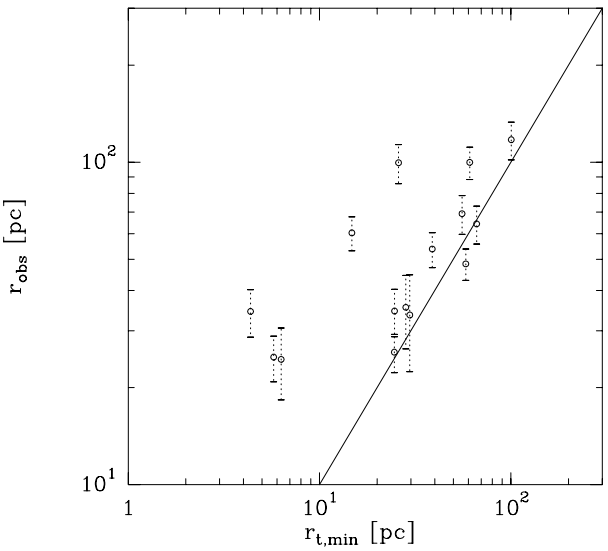

Figure 3. Observed radius $r_{\rm obs}$ versus minimal tidal radius $r_{t,\rm min}$. The line presents a 1:1 relationship.

galaxy and centrifugal force J^2/R^4 from corotation surpasses the own gravitation of the cluster. Thus we can write:

$$r_t(R) \;=\; \frac{2}{3}\sqrt[3]{\frac{G\,M_{\rm cl}}{-\frac{\partial^2\Phi}{\partial R^2}+\frac{J^2}{R^4}}} \qquad (1)$$

where the factor 2/3 takes care for the nonspherical boundary but is insignificant with respect to our errors. Such theoretical radii can be compared with the observed radii $r_{\rm obs}$ from fitting a King formula (or an equivalent one) to the surface brightness function in dependence on r. They are supposed to be tidally determined; therefore also they are often called tidal radii. We will not follow this custom in order to better distinguish the two.

The most obvious expectation is the following one: $r_{\rm obs}$ is determined by the strongest stripping off, i.e. by the minimal value $r_{t,\rm min}$ of r_t occuring near to the perigalacticon of the orbit. Figure 3 shows that there is a correlation between $r_{\rm obs}$ and $r_{t,\rm min}$ and that the order of magnitudes agree. Nevertheless, the ratios vary by one order of magnitude and even changing the numerical factor in Equation 1 would just shift the disagreement from one place to the other. So our expectation is certainly not the full truth. Another assumption to check could be this: $r_{\rm obs}$ originates from a very fast adjustment of the cluster to the forces, i.e. it is rather the instantaneous value $r_t(R_{\rm present}) = r_{t,\rm pres}$. Figure 4 exhibits again a certain correlation but not a satisfying description. Finally, the contrasting hypothesis: the cluster radii adapt very slowly and the observed $r_{\rm obs}$ is the result of an averaged or integrated action over the whole orbit. The best description of such an integration will come from a theoretical understanding. For the time being, we present in Figure 4 the ratio $r_{\rm obs}/r_{t,\rm min}$ as a function of $R_{\rm max}/R_{\rm min}$, the latter characterizing in a first order manner the variations within the orbit. This is a possible description of the data within error limits, in other words, it is possible to assume that

Table 2. Tidal radii.

NGC	$\log(\frac{M}{M_\odot})$	$r_{\rm obs}$	r_t		
			minimal	present	extremal
		[pc]		[pc]	
104	6.03	48	58	103	109
362	5.45	35	4	87	105
4147	4.39	34	30	59	72
5024	5.68	118	100	128	267
5272	5.81	100	61	116	188
5466	4.85	100	26	70	211
5904	5.66	61	15	71	192
6205	5.59	54	39	69	191
6218	5.07	25	6	39	52
6254	5.06	26	25	37	40
6341	5.34	35	25	76	79
6779	4.98	25	6	57	73
6934	5.06	36	28	58	176
7078	5.85	65	66	94	245
7089	5.78	70	56	87	370

$r_{\rm obs}$ is an 'average' tidal radius, whereby the averaging produces approximately the observed function of $R_{\rm max}/R_{\rm min}$.

Such a statement does not exclude a small temporal variation of $r_{\rm obs}$ within errror limits, say a factor of two. N-body calculations have shown that the stripping-off is mainly a diffusion of the high-energy tail of the cluster stars (H. Baumgardt, private communication). The repopulation of this part of the distribution is then a process with a relaxation time scale and these time scales are longer than the revolution times of the clusters around the Galaxy. Within such a picture, the resulting cluster radius would be rather constant along the orbit.

A more detailed account will be given elsewhere by Odenkirchen et al. (in preparation).

ACKNOWLEDGMENTS

We acknowledge gratefully the financial support by the Bundesministerium für Forschung und Technologie (FKZ 50 009101). MO also thanks the European Community for being supported by a Marie Curie postdoctoral fellowship (ERBFMBICT961511).

REFERENCES

Allen C., Santillan A., 1991, Rev. Mex. AA, 22, 255

Brosche P., Tucholke H.-J., Klemola A.R., Ninkovic S., Geffert M., Doerenkamp P., 1991, AJ, 102, 1022

Geffert, M., Hiesgen, M., Colin, J., Dauphole, B., Ducourant, C., 1997, ESA SP–402, this volume

Mandushev G., Spassova N., Staneva A., 1991, A&A, 252, 94

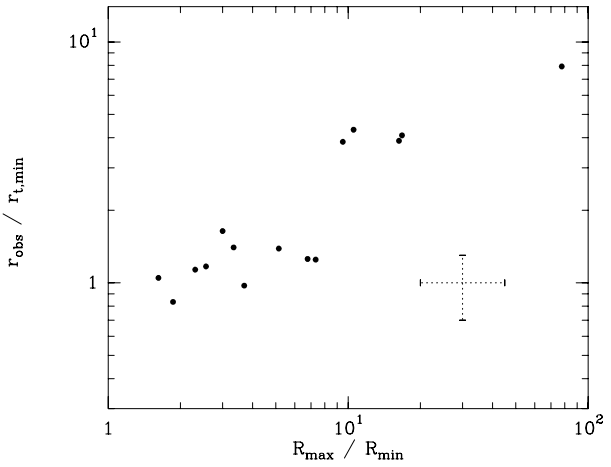

Figure 4. Ratio $r_{\rm obs}/r_{t,\rm min}$ versus galactocentric distance ratio $R_{\rm max}/R_{\rm min}$. The typical size of the errors is indicated by the cross.

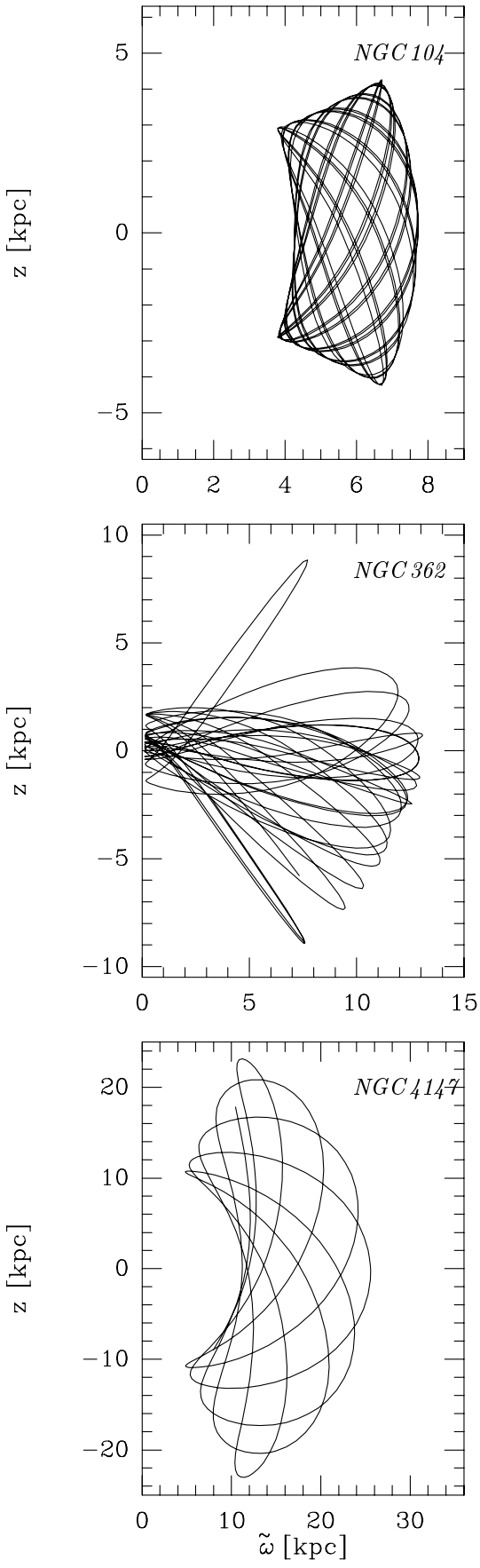

Figure 5. Meridional sections of the orbits.

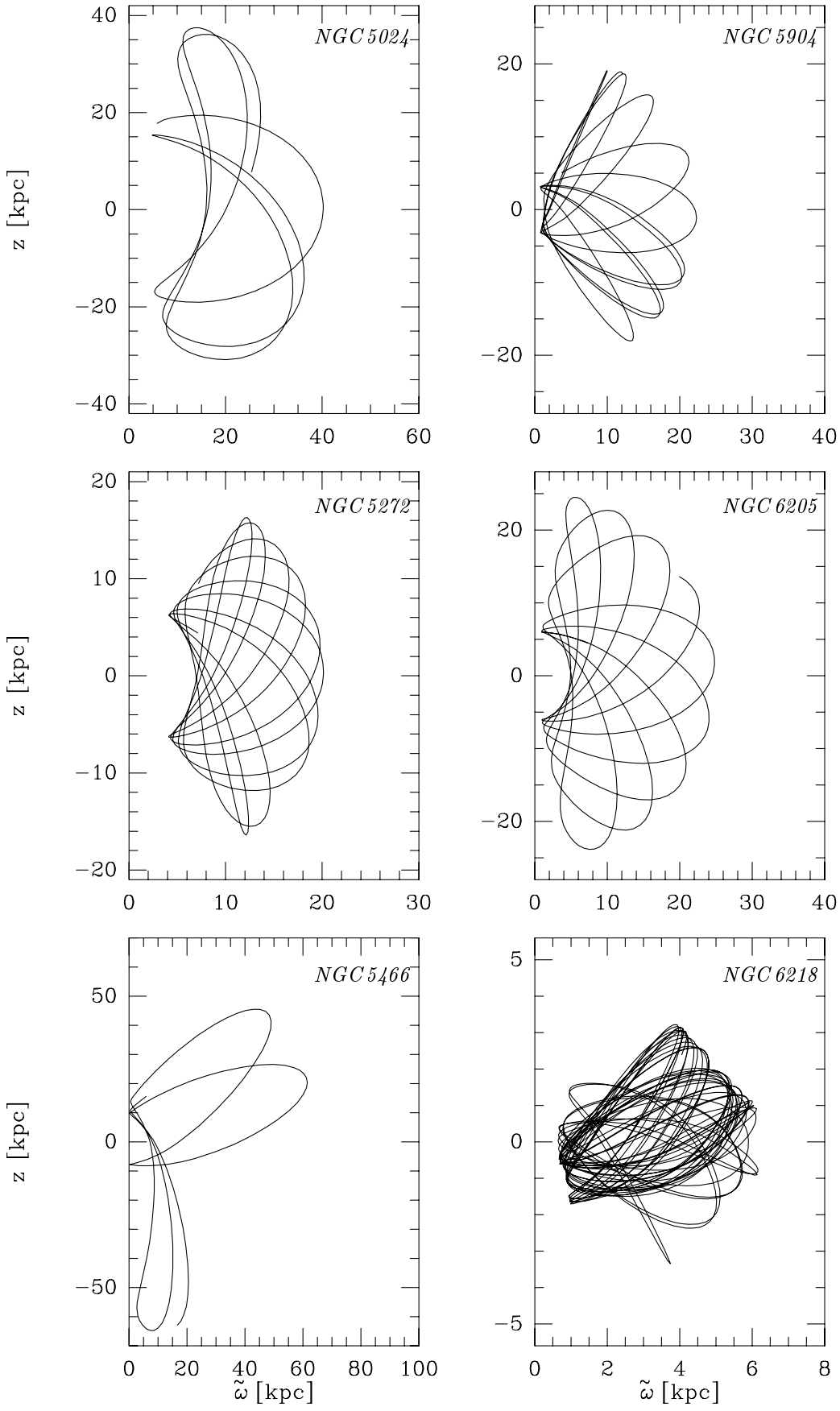

Figure 5. (continued).

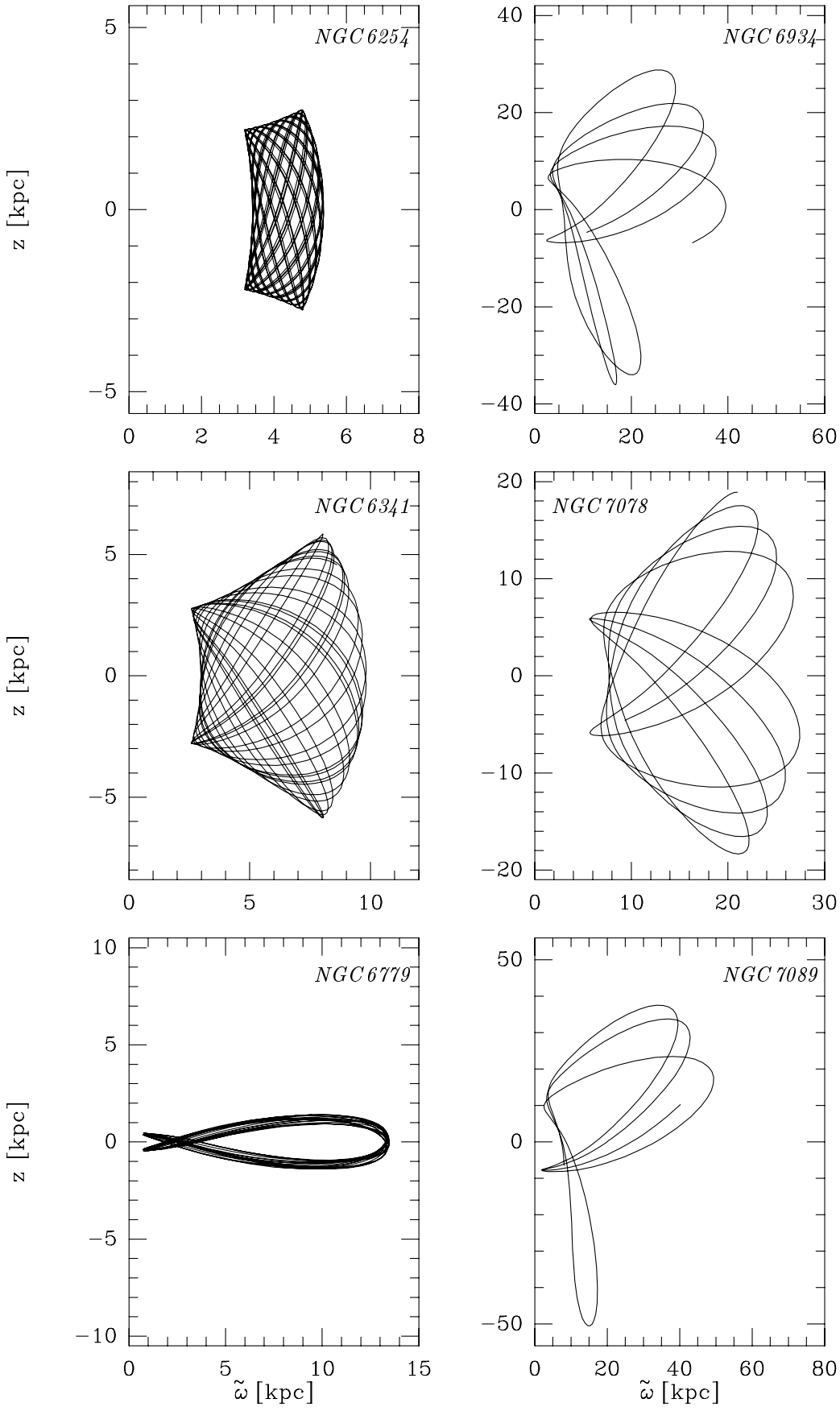

Figure 5. (continued).